

DISCLAIMER

This paper was submitted to the *Memórias do Instituto Oswaldo Cruz* on 3 May 2020 and was posted to the Fast Track site on 13 May 2020. The information herein is available for unrestricted use, distribution and reproduction provided that the original work is properly cited as indicated by the Creative Commons Attribution licence (CC BY).

RECOMMENDED CITATION

da Silva FMA, da Silva KPA, de Oliveira LPM, Costa EV, Koolen HHF, Pinheiro MLB, et al. Flavonoid glycosides and their putative human metabolites as potential inhibitors of the SARS-CoV-2 main protease (Mpro) and RNA-dependent RNA polymerase (RdRp) [Submitted]. Mem Inst Oswaldo Cruz E-pub: 13 May 2020.doi: 10.1590/0074-02760200207.

Original Article

Flavonoid glycosides and their putative human metabolites as potential inhibitors of the SARS-CoV-2 main protease (Mpro) and RNA-dependent RNA polymerase (RdRp)

Felipe Moura A. da Silva^{1*}, Katia Pacheco A. da Silva², Luiz Paulo M. de Oliveira¹, Emmanoel V. Costa³, Hector H. F. Koolen⁴, Maria Lúcia B. Pinheiro¹, Antonia Queiroz L. de Souza^{1,5}, Afonso Duarte L. de Souza^{1,3*}

¹
Central Analítica - Centro de Apoio Multidisciplinar (CAM), Universidade Federal do Amazonas (UFAM), Manaus, AM, Brasil

²
Secretaria Municipal de Saúde, Prefeitura de Itabirito, 35450-000, Itabirito, MG, Brasil

³
Departamento de Química, Universidade Federal do Amazonas (UFAM), Manaus, AM, Brasil

⁴
Grupo de Pesquisa em Metabolômica e Espectrometria de Massas, Universidade do Estado do Amazonas, Manaus, AM, Brasil

⁵
Faculdade de Ciências Agrárias, Universidade Federal do Amazonas (UFAM), Manaus, AM, Brasil

ABSTRACT

BACKGROUND - Since the World Health Organization (WHO) declared COVID-19 to be a pandemic infection, important SARS-CoV-2 non-structural proteins (nsp) have been analysed as promising targets in virtual screening approaches. Among these proteins, 3-chymotrypsin-like cysteine protease (3CLpro), also named main protease, and the RNA-dependent RNA polymerase (RdRp), have been identified as the main targets.

OBJECTIVES - To investigate, *in silico*, the main flavonoid glycosides from *Dysphania ambrosioides*; a medicinal plant found in many regions of the world, along with some of the putative derivatives of these flavonoid glycosides in the human organism as potential inhibitors of the SARS-CoV-2 3CLpro and RdRp.

METHODS - Using a molecular docking analysis, the interactions and the binding affinity with SARS-CoV-2 3CLpro and RdRp were predicted for quercetin-3-*O*-rutinoside (rutin), kaempferol-3-*O*-rutinoside (nicotiflorin) and some of their glucuronide and sulfate derivatives.

FINDINGS - Docking analysis, based on the crystal structure of 3CLpro and RdRp, indicated rutin, nicotiflorin, and their glucuronide derivatives to be the best inhibitors for both proteins. Also, the importance of the hydrogen bond and π -based interactions was evidenced for the presumed active sites.

MAIN CONCLUSIONS - Overall, these results suggest that both flavonoid glycosides and their putative human metabolites can play a key role as inhibitors of the SARS-CoV-2 3CLpro and RdRp. Obviously, further research is necessary to certify the docking results reported here, as well as the adequate application of these substances. Furthermore, it is necessary to investigate the risks of *D. ambrosioides* as a phytomedicine for use against COVID-19.

Keywords:

COVID-19; rutin; nicotiflorin; glucuronides; *Dysphania ambrosioides*; phytomedicines

INTRODUCTION

Since the appearance of the first cases, reported in December 2019 in Wuhan, China, the new pandemic disease COVID-19 caused by coronavirus SARS-CoV-2 has

claimed millions of victims and caused hundreds of deaths around the world. Forthwith, Chinese teams sequenced SARS-CoV-2⁽¹⁾ and its important nonstructural proteins (nsp) were revealed, which included spike proteins, 3-chymotrypsin-like cysteine protease (3CLpro), also named main protease (Mpro), papain-like protease (PLpro), and RNA-dependent RNA polymerase (RdRp).⁽²⁾ The spike proteins bind the virus to the human receptor – a metalloproteinase named angiotensin-converting enzyme 2 (ACE2), while the 3CLpro and the PLpro provide components for packaging new virions from large viral polyproteins translated on host ribosome, and finally the RdRp replicates the SARS-CoV-2 RNA genome.⁽²⁾ Many computational reports based on virtual screening have been done on the inhibition of one or more of these SARS-CoV-2 key proteins, mainly 3CLpro and RdRp, most using drugs used against other human diseases or compounds which have been previously described in medicinal plants.^(3,4) Fortunately, some of these therapeutic medicinal plants, such as *Dysphania ambrosioides* (L.) Mosyakin & Clemants (Syn. *Chenopodium ambrosioides* L.), are commonly found in tropical and subtropical regions and are therefore accessible as therapeutic agents. *D. ambrosioides* is popularly known in Brazil as “mastruz” or “Erva-de-Santa-Maria” and has been used to treat a number of health problems, such as infections, sinusitis, gastritis, inflammations, and flu.^(5,6) From the phytochemical viewpoint, this species is a promising source of flavonoid glycosides.⁽⁷⁾ These glycosides present great biological potential, including antioxidant and antiviral activities, and are vital in diets.⁽⁸⁾ Since *D. ambrosioides* and several other flavonoid-producing sources are used worldwide, the absorption, metabolism and pharmacokinetics of flavonoids have been intensively investigated, and glucuronide and sulfates can be highlighted as important metabolite products in this process.^(9,10) Thus, in the present study, we screened the main flavonoid glycosides from *D. ambrosioides* along with some of their putative derivatives

in the human organism using molecular docking, in order to test them as potential inhibitors of the SARS-CoV-2 3CLpro and RdRp.

MATERIALS AND METHODS

Ligand preparation—Initially, the three-dimensional (3D) structures of quercetin-3-*O*-rutinoside (rutin), quercetin-3-*O*-glucuronide, quercetin-3'-*O*-sulfate, and quercetin were downloaded from ZINC database (<http://zinc15.docking.org/>) as SDF files. These files were used as templates to generate, via Marvin Sketch software (<https://chemaxon.com/products/marvin>), kaempferol-3-*O*-rutinoside (nicotiflorin), kaempferol, and some of their putative mono-glucuronide and sulfated derivatives (Figure 1), based on previous pharmacokinetic studies on the human organism.^(9,10) Also, theaflavin, a phenolic compound suggested as potential SARS-CoV-2 RdRp inhibitor,⁽¹¹⁾ was downloaded from ZINC database. Subsequently, all the structures were subjected to geometry optimization by the semi-empirical method PM7 using MOPAC2016 software (<http://openmopac.net/MOPAC2016.html>), being the results saved as PDB files. Finally, the ligands were prepared via Autodocktools⁽¹²⁾ and saved as PDBQT files.

Protein preparation—The 3D crystal structures of the SARS-CoV-2 3CLpro (PDB ID: 6W63) and RdRp (PDB ID: 6M71) were retrieved from Research Collaboratory for Structural Bioinformatics Protein Data Bank (RCSB PDB) (<http://www.rcsb.org>) as PDB files. These receptors were prepared via Autodock tools and saved as PDBQT files.

Docking Simulations– The docking simulations were as previously reported,⁽¹³⁾ in which the grid box was centered at the ligand X77 in 3CLpro (PDB ID: 6W63) and at the presumed active site^(11,14) in the RdRp (PDB ID: 6M71). The interactions and the binding affinity of the protein-ligand complex were predicted via a rigid docking process using AutodockVina⁽¹⁵⁾ and viewed with the Discovery Studio software.⁽¹⁶⁾ Due to the lack of models with ligands for RdRp in the RCSB PDB, only the 3CLpro was tested for redocking.

RESULTS

Molecular docking with 3CLpro (main protease– Mpro)– Docking analysis revealed scoring function values for nicotiflorin (-11.2 kcal/mol) and rutin (-10.3 kcal/mol) close to that obtained for the previously described inhibitor X77 (redocking binding free energy = -12.4 kcal/mol, RMSD < 2) when docked with 3CLpro, which suggests the establishment of favorable interactions for the ligand-3CLpro complex.

The putative human metabolites from rutin, quercetin-7-*O*-glucuronide (-10.9 kcal/mol) and quercetin-3-*O*-glucuronide (-10.7 kcal/mol) presented better binding free energy than its precursors, while quercetin-3'-*O*-glucuronide (-10.2 kcal/mol) was close to this result. On the other hand, the quercetin sulfates (-9.2 to -9.5 kcal/mol) presented worse binding free energy than the glucuronides derivatives, irrespective of the sulfate's position. For quercetin, the binding free energy of -8.3 kcal/mol observed was the worst among the putative human metabolites from rutin. Regarding the putative metabolites from nicotiflorin, the 7-glucuronide derivative (-10.9 kcal/mol) also presented the best scoring function value among the kaempferol glucuronide derivatives, followed by kaempferol-4'-*O*-glucuronide (-9.7 kcal/mol). Surprisingly, the kaempferol-3-*O*-glucuronide (-9.1 kcal/mol) presented binding free energy slightly worse

thankaempferol-3-*O*-sulfate (-9.4 kcal/mol). Similarly to quercetin, kaempferol (-8.1 kcal/mol) presented worst binding free energy than all its chemical derivatives.

In regards to the observed interactions in the presumed active site of 3CLpro, hydrogen bonds and π -based interactions, such as π -sulfur, π -alkyl, π - π , and π -cation interactions, were dominant in almost all tested compounds (Table 1). The interactions observed for quercetin-7-*O*-glucuronide, the compounds with the best scoring function value in the quercetin-set, were hydrogen bonds with the residues Thr26, Gln189, and Glu166, π - π and π -cation interaction with His41, and π -alkyl interaction with Met49 (Figure 2). The second best inhibitor of the quercetin-set, quercetin-3-*O*-glucuronide, presented hydrogen bonds with Thr25, Cys44, Asn142, Ser144, His163, Met165, Glu166, and Arg188, and π -alkyl interaction with Met49 and Met165 (Figure 2). However, rutin, the third best inhibitor of the quercetin-set, also presented some hydrogen bonds, along with π - π and π -cation interactions with His41 and π -alkyl interaction with Met49 (Figure 2). On the other hand, nicotiflorin, the compound with the best scoring function values in kaempferol-set, presented, besides hydrogen bonds, important π - π and π -cation interactions with His41 and π -alkyl interaction with Met49. Similar interactions were observed for kaempferol-7-*O*-glucuronide, the second of the kaempferol-set (Figure 2). The main observed interactions between the vegetal flavonoid glycosides and their putative human metabolites with 3CLpro are summarized in Table 1.

Molecular docking for RNA-dependent RNA polymerase (RdRp)—Docking analysis using RdRp revealed better scoring function values for rutin (-11.7 kcal/mol) and nicotiflorin (-11.3 kcal/mol) than for theaflavin (-11.2 kcal/mol) (Table 1).

Similarly to the results observed in docking with 3CLpro, the glucuronide derivatives (quercetin = -10.2 to -10.5 kcal/mol; kaempferol = -10.0 to -10.2 kcal/mol) also presented better binding free energy than sulfate derivatives (quercetin = -8.8 to -9.4 kcal/mol; kaempferol = -8.7 to -9.3 kcal/mol), with aglycones again presenting the worst binding free energies (quercetin = -8.2 and kaempferol = -7.7 kcal/mol) with RdRp.

Regarding to the observed interactions in the presumed active site of RdRp, hydrogen bonds, π -cation and π -anion interactions were dominant to almost all tested compounds (Table 1). Since this active site includes the motif A (residues 611-626), with the classic divalent cation-binding residue 618, and motif C (residues 753-767), with the catalytic residues 759-761⁽¹⁴⁾, we therefore focused our interpretation on these interactions. The observed interactions for theaflavin were near to that previously described in the literature,⁽¹¹⁾ and highlighted the hydrogen bonds observed with Asp623 and Asp760, from motif A and C, respectively, (Figure 3) which is suggestive of a good approximation of the present model with the previous model by homology. Also, for theaflavin, π -anion interactions were observed with Asp760 and Asp761 from motif C. For rutin, the best of the compounds in this study, among the other interactions, key hydrogen bonds were observed with Tyr619 and Lys621 from motif A, and Asp760, from motif C (Figure 3). Similarly, for nicotiflorin hydrogen bonds were observed with those same residues from motif A and C, along with π -anion interaction with Glu811 (Figure 3). The main observed interactions between the flavonoid glycosides and their putative human metabolites with RdRp are summarized in Table 1.

DISCUSSION

Rutin and nicotiflorin, as well as other glycoside flavonoids, are present in a large number of therapeutic medicinal plants and are often consumed in the form of herbal

teas.⁽¹⁷⁾ These compounds are vital in diets and are of great interest due to their antioxidant, anti-inflammatory and antiviral activities and their human metabolites, which include quercetin from rutin hydrolysis.^(8,17-20) For this reason, their absorption, metabolism, toxicity, and pharmacokinetics has been intensively investigated.^(9,10) Regarding these studies, rutinoid flavonoids, such as rutin and nicotiflorine, are deglycosylated prior to being absorbed into the circulation and then conjugated mainly with glucuronate and sulfate, these being the main forms in plasma.⁽⁹⁾ Based on this information, it is reasonable to suggest that both quercetin and kaempferol glucuronides, demonstrated above as promising 3CLpro and RdRp inhibitors, could have a key role against these proteins, since the virus is also dominant in plasma. This hypothesis is in accordance with previous *in vivo* antiviral studies performed with rutin. These studies indicate that rutin protects cells for about 24 h against vesicular stomatitis virus, affords immense viral embarrassment in canine distemper virus, and demonstrates a profound antiviral effect against avian influenza strain H5N1.⁽⁸⁾ Flavonoid glucuronides have also been described as antiviral agents, including quercetin-3-*O*-glucuronide, here described as a potential 3CLpro inhibitor.^(21,22) On the other hand, although sulfate products have not showed high binding free energy compared to glucuronides in docking analysis, their antiviral potential should also be considered, since previous works have pointed out their effective anti-HIV and – HSD activities.⁽²³⁾

Recent autopsy studies have permitted Brazilian COVID-19 patients to be treated as sufferers of Dissemination Intravascular of Coagulum (DIC), which can cause failure of several organs, mainly the lungs.⁽²⁴⁾ As a preliminary stage for combating the disease, Low Molecular Weight Heparin (LMWH) has been successfully administered.⁽²⁵⁾ In addition to its anticoagulant therapeutic effects, LMWH has demonstrated anti-

inflammatory effects, endothelial protection and viral inhibition.⁽²⁶⁾ Rutin, displayed here as an active agent against 3CLpro and RdRp of SARS-CoV-2, has also proved to have anticoagulant therapeutic effects⁽²⁷⁾ as well as anti-inflammatory effects and potential protection against acute lung injury (ALI).⁽²⁸⁾ Intravenous or intranasal administration could be an alternative to oral intake, thus improving its bioavailability.^(29,30) *D. ambrosioides* has been used successfully by the riverside population in the Amazon region for treating cases of acute respiratory distress syndrome (ARDS) and tuberculosis. These results may also be related to the presence of rutin.⁶

Overall, these results suggest that rutin, nicotiflorin, and their putative human metabolites, mainly glucuronides, but also sulfates, can play a key role as inhibitors of the SARS-CoV-2 3CLpro and RdRp. Such derivatives, which are expected in plasma, are in fact the most likely compounds for targeting these viral proteins, via oral intake of these flavonoid glycosides. However, at least for rutin, intravenous or intranasal administration can be an alternative for prompt bioavailability. Our results, and much of the reported data, suggest rutin and nicotiflorin as possible alternatives for combating the COVID-19 virus. Rutin could even be considered an alternative to LMWH, given its anticoagulant and anti-inflammatory effects and its potential protection against ALI. Obviously, further research is necessary to corroborate the docking results reported here, as well as the adequate application of these substances. Furthermore, it is necessary to investigate the risks of *D. ambrosioides* as a phytomedicine for use against COVID-19.

ACKNOWLEDGMENTS

The authors are grateful to Capes, CNPq, and FAPEAM for preliminary support.

AUTHOR CONTRIBUTIONS

FMAS: Conceptualization, Methodology, Formal analysis, Data Curation, Writing - Original Draft. KPAS: Conceptualization, Investigation. LPMO: Investigation. EVC: Investigation. HHFK: Investigation. MLBP: Conceptualization, Investigation. AQLS: Conceptualization, Investigation, Writing - Original Draft. ADLS: Conceptualization, Methodology, Formal analysis, Data Curation, Writing - Original Draft, Supervision.

REFERENCES

1. Zhu N, Zhang D, Wang W, Li X, Yang B, Song J, et al. A novel coronavirus from patients with pneumonia in China, 2019. *N Engl J Med.* 2020; 382: 727-733.
2. Morse JS, Lalonde T, Xu S, Liu WR. Learning from the past: possible urgent prevention and treatment options for severe acute respiratory infections caused by 2019-nCoV. *ChemBioChem.* 2020; 21: 730-738.
3. Qamar MT, Alqahtani SM., Alamri MA., Chen LL. Structural basis of SARS-CoV-2 3CLpro and anti-COVID-19 drug discovery from medicinal plants. *Journal of pharmaceutical analysis.* 2020. <https://doi.org/10.1016/j.jpha.2020.03.009>.
4. Wu C, Liu Y, Yang Y, Zhang P, Zhong W, Wang Y, et al. Analysis of therapeutic targets for SARS-CoV-2 and discovery of potential drugs by computational methods. *[Acta Pharmaceutica Sinica] B.* 2020. <https://doi.org/10.1016/j.apsb.2020.02.008>.
5. Trivellato Grassi L, Malheiros A, Meyre-Silva C, Buss ZS, Monguilhott ED, Frode TS, et al. From popular use to pharmacological validation: a study of the anti-

- inflammatory, anti-nociceptive and healing effects of *Chenopodium ambrosioides* extract. *J Ethnopharmacol.* 2013; 145: 127-138.
6. Ribeiro, RV, Bieski IGC, Balogun SO, Martins DTO. Ethnobotanical study of medicinal plants used by Ribeirinhos in the North Araguaia microregion, Mato Grosso, Brazil. *J Ethnopharmacol.* 2017; 205: 69-102.
7. Barros L, Pereira E, Calhella RC, Dueñas M, Carvalho AM, Santos-Buelga C, et al. Bioactivity and chemical characterization in hydrophilic and lipophilic compounds of *Chenopodium ambrosioides* L. *Journal of Functional Foods.* 2013; 5: 1732-1740.
8. Ganeshpurkar A, Saluja AK. The pharmacological potential of rutin. *Saudi Pharmaceutical Journal.* 2017; 25: 149-164.
9. Manach C, Donovan J. Pharmacokinetics and metabolism of dietary flavonoids in humans. *Free Radic Res.* 2004; 38: 771-785.
10. Barrington R, Williamson G, Bennett RN, Davis BD, Brodbelt JS, Kroon PA. Absorption, conjugation and efflux of the flavonoids, kaempferol and galangin, using the intestinal CaCo-2/TC7 cell model. *Journal of Functional Foods.* 2009; 1: 74-87.
11. Lung J, Lin YS, Yang YH, Chou YL, Shu LH, Cheng YC, et al. The potential chemical structure of anti-SARS-CoV-2 RNA-dependent RNA polymerase. *J Med Virol.* 2020. <https://doi.org/10.1002/jmv.25761>.
12. Morris GM, Huey R, Lindstrom W, Sanner MF, Belew RK, Goodsell DS, et al. AutoDock4 and AutoDockTools4: automated docking with selective receptor flexibility. *Journal of Computational Chemistry.* 2009; 30: 2785-2791.
13. Lima BR, Lima JM, Maciel JB, Valentim CQ, Nunomura RCS, Lima ES, et al. Synthesis and inhibition evaluation of new

- benzyltetrahydroprotoberberine alkaloids designed as acetylcholinesterase inhibitors. *Frontiers in Chemistry*. 2019; 7: 629.
14. Gao Y, Yan L, Huang Y, Liu F, Zhao Y, Cao L, et al. Structure of the RNA-dependent RNA polymerase from COVID-19 virus. *Science*. 2020. Doi:10.1126/science.abb7498.
15. Trott O, Olson AJ. AutoDock Vina: improving the speed and accuracy of docking with a new scoring function, efficient optimization, and multithreading. *Journal of Computational Chemistry*. 2010; 31: 455-461.
16. Discovery Studio Visualizer, V 16.1.0, Accelrys Inc, San Diego, CA, 2016.
17. Chua LS. A review on plant-based rutin extraction methods and its pharmacological activities. *J Ethnopharmacol*. 2013; 140: 805-817.
18. Xiao J. Dietary flavonoid aglycones and their glycosides: Which show better biological significance? *Critical Reviews in Food Science and Nutrition*. 2017; 57: 1874-1905.
19. Kaul TN, Middleton-Junior E, Ogra PL. Antiviral effect of flavonoids on human viruses. *J Med Virol*. 1985; 15: 71-79.
20. Wu W, Li R, Li X, He J, Jiang S, Liu S, et al. Quercetin as an antiviral agent inhibits influenza A virus (IAV) entry. *Viruses*. 2016; 8: 6.
21. Lee JS, Kim HJ, Lee YS. A new anti-HIV flavonoid glucuronide from *Chrysanthemum morifolium*. *Planta Med*. 2003; 69: 859-861.
22. Fan D, Zhou X, Zhao C, Chen H, Zhao Y, Gong X. Anti-inflammatory, antiviral and quantitative study of quercetin-3-O- β -D-glucuronide in *Polygonum perforfoliatum* L. *Fitoterapia*. 2011; 82: 805-810.

23. Tao J, Hu Q, Yang J, Li R, Li X, Lu C, et al. *In vitro* anti-HIV and -HSV activity and safety of sodium rutin sulfate as a microbicide candidate. *Antiviral Res.* 2007; 75: 227-233.
24. Yao XH, Li TY, He ZC, Ping YF, Liu HW, Yu SC, et al. [A pathological report of three COVID-19 cases by minimally invasive autopsies]. [*Chinese Journal of Pathology*]. 2020. 10.3760/cma.j.cn112151-20200312-00193.
25. Negri EM, Piloto B, Morinaga LK, Jardim CVP, Lamy SAED, Ferreira MA, et al.. Heparin therapy improving hypoxia in COVID-19 patients - a case series.. *MedRxiv.* 2020. Doi: 10.1101/2020.04.15.20067017.
26. Thachil, J. The versatile heparin in COVID-19. *Journal of Thrombosis and Haemostasis.* 2020. Doi: 10.1111/jth.14821.
27. Dar MA, Tabassum, N. Rutin- potent natural thrombolytic agent. *International Current Pharmaceutical Journal.* 2012; 1: 431-435.
28. Yeh CH, Yang JJ, Yang ML, Li YC, Kuan YH. Rutin decreases lipopolysaccharide-induced acute lung injury via inhibition of oxidative stress and the MAPK-NF-kappa B pathway. *Free Radical Biology & Medicine.* 2014; 69: 249-257.
29. Ahmad N, Ahmad R, Naqvi AA, Alam MA, Ashafaq M, Samim M, et al. Rutin-encapsulated chitosan nanoparticle targeted to the brain in the treatment of cerebral ischemia. *International Journal of Biological Macromolecules.* 2016; 91: 640-655.
30. Ishak RAH, Mostafa NM, Kamel AO. Stealth lipid polymer hybrid nanoparticles loaded with rutin for effective brain delivery – comparative study with the gold standard (Tween 80): optimization, characterization and biodistribution. *Drug Delivery.* 2017; 24: 1874-1890.

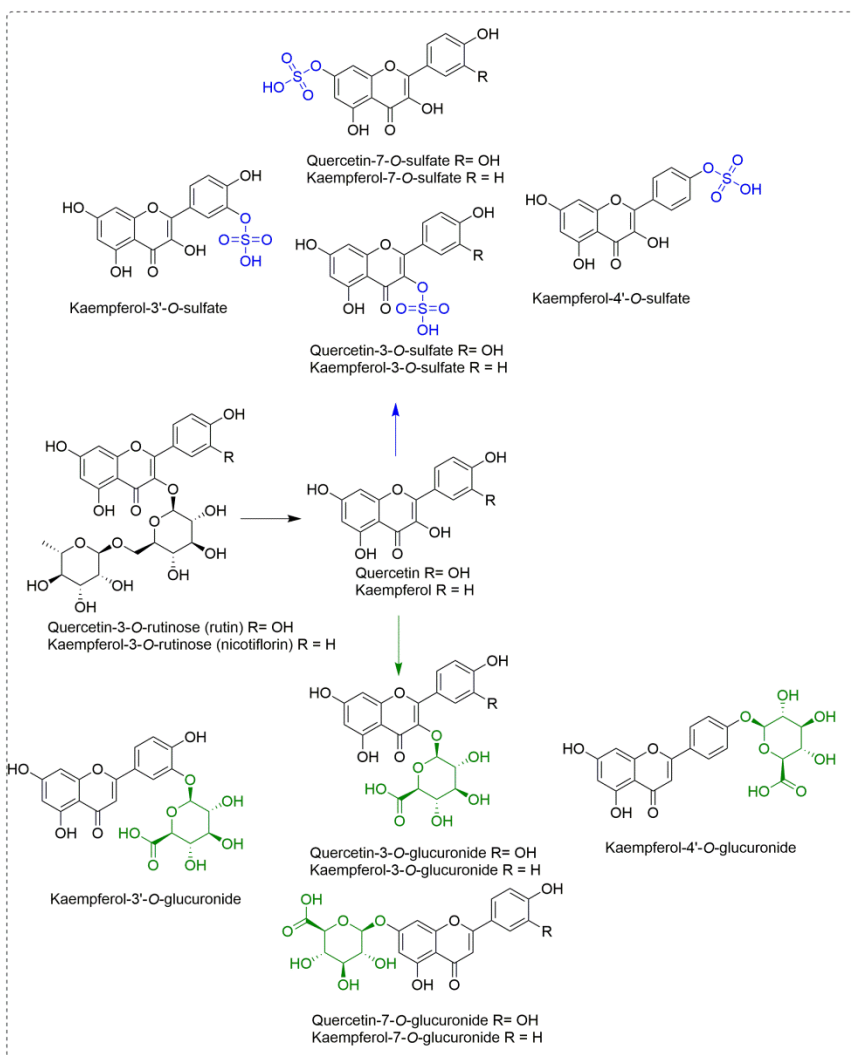


Figure 1. Chemical structures of the main flavonoid glycosides from *D. ambrosioides*, along with some of their putative derivatives in human organism.

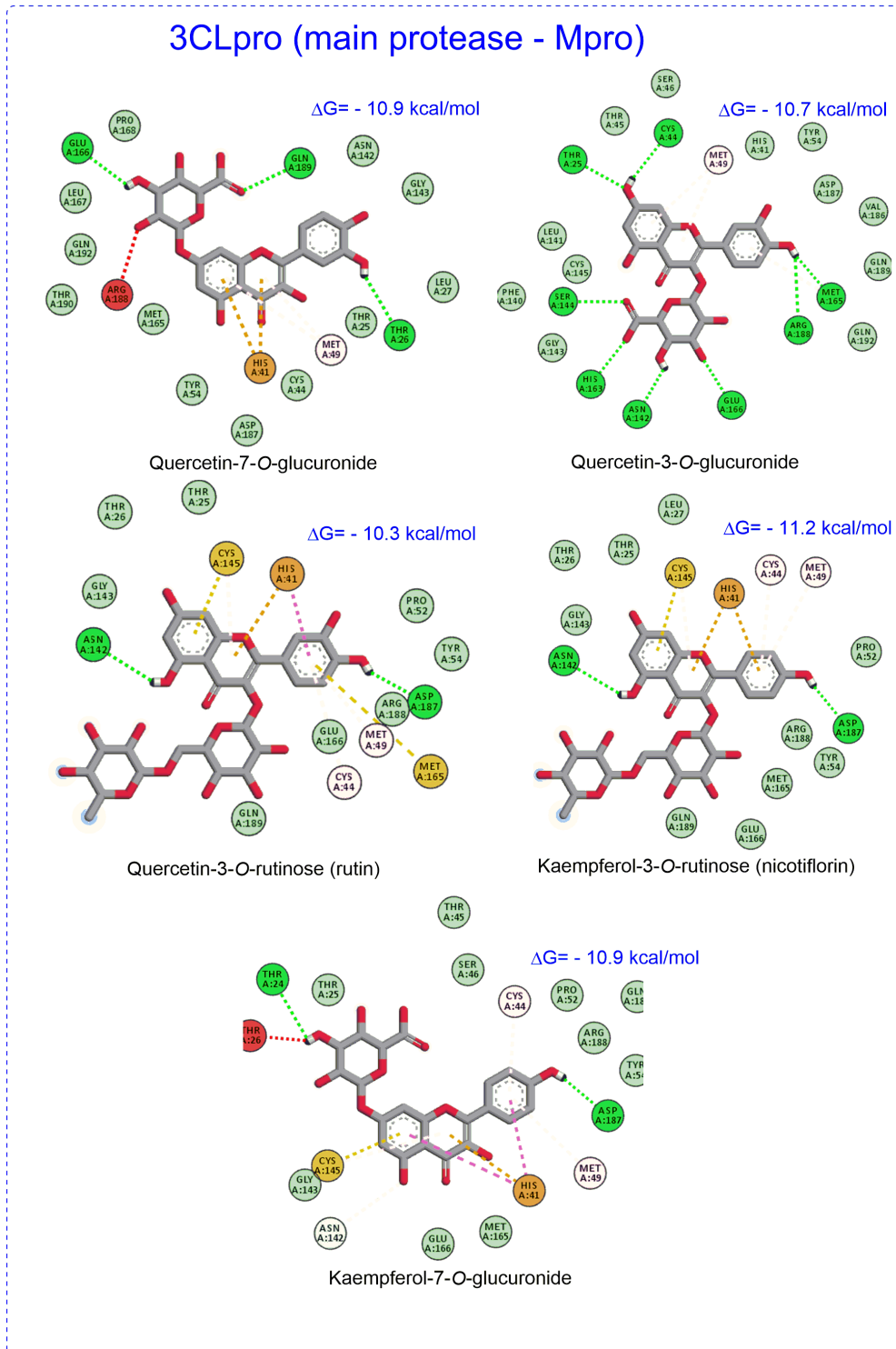


Figure 2. Main interactions observed for the best inhibitors of 3CLpro by docking analysis.

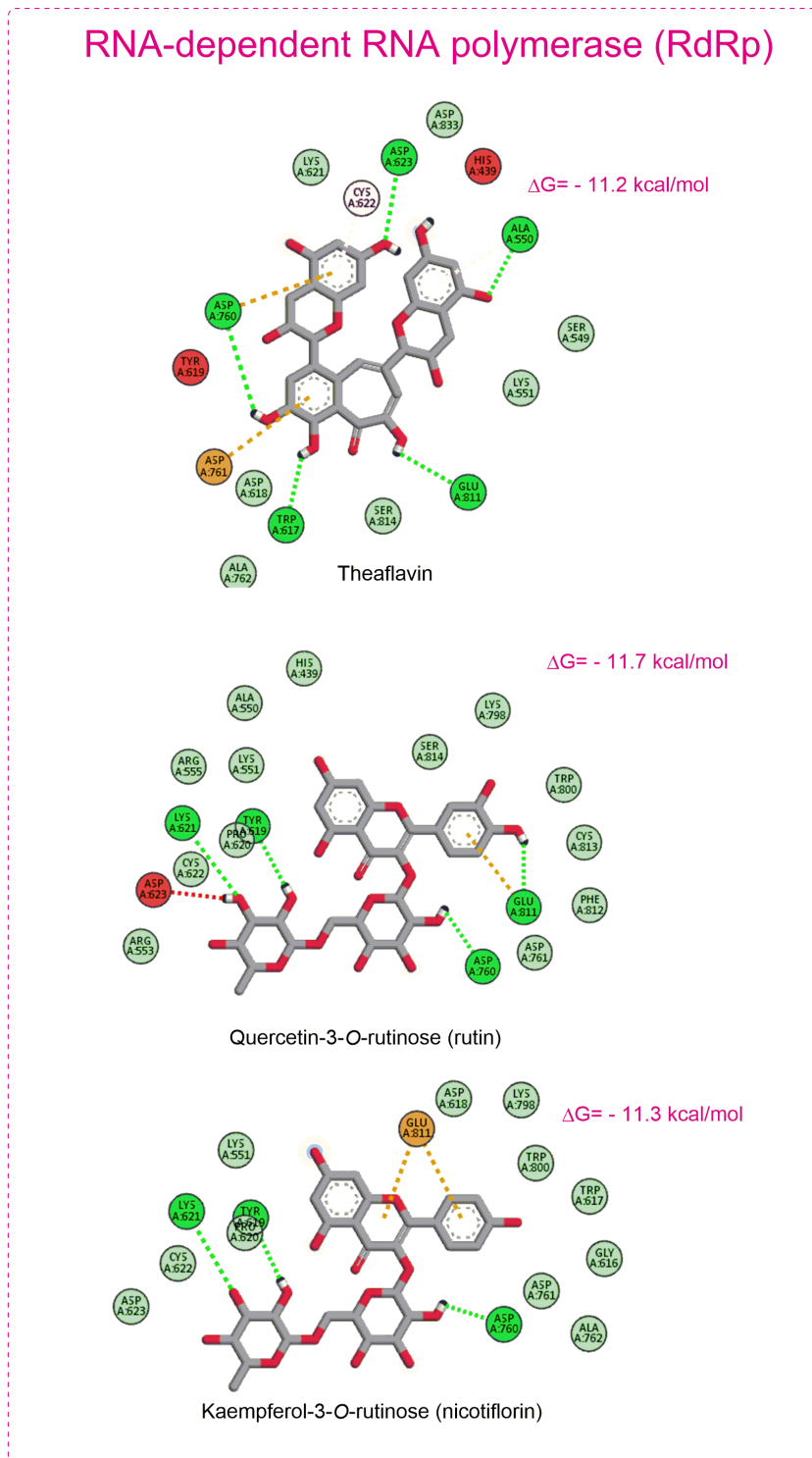


Figure 3. Main interactions observed for theaflavin, rutin and nicotiflorin-RdRp complex by docking analysis.

Table 1. Docking analysis datafor the main flavonoid glycosides from *D. ambrosioides* along with some of their putative derivatives in human organism

Compounds	Protein (PDB iD)	Bindingenergy (kcal/mol)	Maininteractions
Theaflavin	RdRp (7M71)	-11.2	HB (Ala550, Trp617, Aap623, Asp760, Glu811), PA (Asp760, Asp761), PAI (Ala550, Cys622)
x77	3CLpro (6W63)	-12.4	HB (Gly143, Glu166), PS (Met49), PAI (Leu27, His41, Pro168), PAm (Leu 141)
Quercetin-3- <i>O</i> -rutinose (Rutin)	RdRp (7M71)	-11.7	HB (Tyr619, Lys621, Asp760, Glu811), PA (Glu811)
	3CLpro (6W63)	-10.3	HB (Asn142, Asp187), PS (Cys145, Met165), PP (His41), PC (His41), PAI (Cys44, Met49, Cys145)
Quercetin-7- <i>O</i> -glucuronide	RdRp (7M71)	-10.5	HB (Arg553, Ser549, Tyr619, Trp800, Glu811, Cys813), PC (ARG555, LYS551)
	3CLpro (6W63)	-10.9	HB (Thr26, Glu166, Gln189), PP (His41), PC (His41), PAI (Met49)
Quercetin-3'- <i>O</i> -glucuronide	RdRp (7M71)	-10.5	HB (Cys622, Asp623, Asp760, Glu811, Cys813, Ser814), PA (Asp618, Asp761)
	3CLpro (6W63)	-10.2	HB (Gly143, His164), PAI (Met49)
Quercetin-3- <i>O</i> -glucuronide	RdRp (7M71)	-10.2	HB (Thr556, Tyr619, Lys621, Thr687, Asn691, Ser759, Asp760), PC (Arg555, Arg553), PA (Asp623), PAI (Lys621)
	3CLpro (6W63)	-10.7	HB (Thr25, Cys44, Asn142, Ser144, His163, Met165, Glu166, Arg188), PAI (Met49, Met165)
	RdRp (7M71)	-9.4	HB (Lys545, Lys621, Arg624), PC (Arg555, Arg553), PA (Asp623), PAI (Arg 624)
Quercetin-7- <i>O</i> -sulfate	RdRp (7M71)	-9.4	HB (Lys545, Lys621, Arg624), PC (Arg555, Arg553), PA (Asp623), PAI (Arg 624)
	3CLpro (6W63)	-9.5	HB (Thr25, Ser144, Glu166), PS (Cys145), PC (His41), PAI (Met49, Met165)
Quercetin-3- <i>O</i> -sulfate	RdRp (7M71)	-8.8	HB (Asp452, Arg553, Thr556, Tyr619), PC (Arg553), PA (Asp623)
	3CLpro (6W63)	-9.5	HB(Asn142, Thr190), PS (Met165), PSi (Gln189), PAI (Met165)
Quercetin-3'- <i>O</i> -sulfate	RdRp (7M71)	-8.8	HB (Ser814), PA (Asp760, Asp761)
	3CLpro (6W63)	-9.2	HB (Met49, Gly143, Asp187), PSi (Thr25), PP (His41), PC (His41), PAI (Cys44, Met49)
Quercetin	RdRp (7M71)	-8.2	HB (Asp760, Trp800), PA (Asp761)
	3CLpro (6W63)	-8.3	HB (Glu166), PS (Met49), PC (His41), PAI (Met165)
Kaempferol-3- <i>O</i> -rutinose (Nicotiflorin)	RdRp (7M71)	-11.3	HB (Tyr619, Lys621, Asp760), PA (Glu811)
	3CLpro (6W63)	-11.2	HB (Asn142, Asp187), PP (His41), PS (Cys145), PC (His41), PAI (Cys44, Met49, Cys145)
Kaempferol-4'- <i>O</i> -glucuronide	RdRp (7M71)	-10.2	HB (Asp618, Lys621, Asp623, Asp761), PA (Glu811)
	3CLpro (6W63)	-9.7	HB (Thr24, Cys44), PS (Met49), PP (His41), PAI (Cys44, Met49)
Kaempferol-3- <i>O</i> -glucuronide	RdRp (7M71)	-10.1	HB (Tyr619, Asp760, Asp761, Glu811, Cys813)
	3CLpro (6W63)	-9.1	HB (Asn142, Glu166), PP (His41), PC (His41), PAI (Cys44, Met49)
Kaempferol-7- <i>O</i> -glucuronide	RdRp (7M71)	-10.0	HB (Asp760, Trp800), PA (Glu811), PAI (Lys798)
	3CLpro (6W63)	-10.9	HB (Thr24, Asp187), PP (His41), PS (Cys145), PC (His41), PAI (Cys44, Met49, Cys145)
Kaempferol-7- <i>O</i> -sulfate	RdRp (7M71)	-9.3	HB (Lys545, Lys621, Arg624), PC (Arg553, Arg555), PA (Asp623), PAI (Arg624)
	3CLpro (6W63)	-9.1	HB (Gly143, Glu166), PS (Cys145), PP (His41), PC (His41), PAI (Cys44, Met49, Cys145)
Kaempferol-4'- <i>O</i> -sulfate	RdRp (7M71)	-9.2	HB (Arg553, Lys621, Thr687, Asn691), PC (Arg553), PA (Asp623), PS (Cys622), PAI (Lys621)
	3CLpro (6W63)	-9.0	HB (Leu141, His163), PS (Cys145), PP (His41)
Kaempferol-3- <i>O</i> -sulfate	RdRp (7M71)	-8.7	HB (Arg553, Arg555, Thr556, Tyr619, Lys621, Arg624), PC (Arg553), PA (Asp623), PAI (Lys621)
	3CLpro (6W63)	-9.4	HB (Met49, His41, Gly143, Glu166), PS (Cys44, Met49, Cys145), PP (His41), PC (His41), PAI (Cys145)
Kaempferol	RdRp (7M71)	-7.7	HB (Tyr619, Ser814), PA (Asp760, Asp761)
	3CLpro (6W63)	-8.1	HB (Met49, Gly143, Asp187), PS (Cys44, Cys145), PP (His41), PC (His41), PAI (Cys145)

^aHB – hydrogen bond, PS – π -sulfur, PAI – π -alkyl, PP – π - π , PA – π -anion, PC – π -cation, PSi – π -sigma, PAm – π -amide

